IJFAC

Indonesian Journal of Fundamental and Applied Chemistry

Article http://ijfac.unsri.ac.id

Photocatalytic Degradation of Congo Red using Iron Sand-Derived Fe_3O_4: Evaluation of Phytotoxicity of the Treated Solution

Fatma Fatma[1]*, Fahma Riyanti[1], Dwi Hardestyariki[2], Nafisha Yustizia[1], and Poedji Loekitowati Hariani[1]

[1] Department of Chemistry, Faculty of Mathematics and Natural Science, Universitas Sriwijaya, Jl. Raya Palembang Prabumulih KM 32 Indralaya Ogan Ilir

[2] Department of Biology, Faculty of Mathematics and Natural Science, Universitas Sriwijaya, Jl. Raya Palembang Prabumulih KM 32 Indralaya Ogan Ilir

*Corresponding Author: fatmakahar62@gmail.com

Abstract

Iron sand is an abundant natural resource in Indonesia. In this study, Fe_3O_4 was synthesized from iron sand originating from the Tekana River, OKU, South Sumatra, and applied for photocatalytic degradation of Congo red dye (CRD). Fe_3O_4 was synthesized using the coprecipitation method at pH variations of 9, 10, and 11. The characterization results showed that increasing pH resulted in better crystallinity. Fe_3O_4 synthesized at pH 11 had a cubic structure with the smallest crystal size of 28.4 nm and the largest saturation magnetization of 74.66 emu/g. The best Fe_3O_4 was then used for Congo red dye degradation and phytotoxicity testing. Photodegradation optimization was carried out by Response surface methodology (RSM) using Central composite design (CCD) through three independent variables: solution pH, Congo red concentration, and irradiation time. The quadratic model was identified as the most suitable model to describe the degradation process with optimum conditions at pH 4, concentration of 37.5 mg/L, and irradiation time of 62 min, resulting in a degradation efficiency of 98.93%. In addition, Fe_3O_4 showed good stability with a 6.91% decrease in efficiency after five reuse cycles. The results of phytotoxicity tests using *Vigna radiata* seeds showed no significant difference in plant growth using the degraded dye solution media and the control. These results indicate that Fe_3O_4 from iron sand is effective and stable as a photocatalyst, and also safe for the environment.

Keywords: Iron sand, Fe_3O_4, Congo red dye, RSM optimization, phytotoxicity

Article Info

Received 29 March 2026
Received in revised 12 May 2026
Accepted 13 May 2026
Available Online 30 June 2026

Abstrak (Indonesian)

Pasir besi merupakan sumber daya alam yang melimpah di Indonesia. Pada penelitian ini, disintesis Fe_3O_4 dari pasir besi yang berasal dari Sungai Tekana, OKU, Sumatera Selatan dan diaplikasikan untuk degradasi fotokatalitik zat warna Congo red (CRD). Fe_3O_4 disintesis menggunakan metode kopresipitasi pada variasi pH 9, 10, dan 11. Hasil karakterisasi menunjukkan bahwa peningkatan pH menghasilkan kristalinitas yang lebih baik. Fe_3O_4 yang disintesis pada pH 11 memiliki struktur kubik dengan ukuran kristal terkecil yaitu 28,4 nm serta magnetisasi saturasi terbesar yaitu 74,66 emu/g. Fe_3O_4 terbaik ini kemudian digunakan untuk degradasi CRD dan uji fitotoksisitas. Optimasi fotodegradasi dilakukan dengan *Response surface methodology* (RSM) menggunakan desain *Central composite design* (CCD) menggunakan tiga variabel bebas: pH larutan, konsentrasi CRD, dan lama iradiasi. Model kuadratik teridentifikasi sebagai model yang paling sesuai untuk menggambarkan proses degradasi dengan kondisi optimum pada pH 4, konsentrasi CRD 37,5 mg/L, dan lama iradiasi 62 menit, menghasilkan efisiensi degradasi sebesar 98,93%. Selain itu, Fe_3O_4 menunjukkan stabilitas yang baik dengan penurunan efisiensi 6,91% setelah lima siklus penggunaan ulang. Hasil uji fitotoksisitas menggunakan biji kacang hijau menunjukkan tidak adanya perbedaan siginifikan pertumbuhan tanaman

menggunakan media larutan zat warna yang telah didegradasi dan kontrol. Hasil ini menunjukkan bahwa Fe_3O_4 yang disintesis dari pasir besi efektif dan stabil sebagai fotokatalis, serta aman bagi lingkungan.

Kata Kunci: Pasir besi, Fe_3O_4, zat warna Congo red, Optimasi RSM, fitotoksisitas

INTRODUCTION

Iron sand is one of the abundant mineral resources, especially in coastal areas such as South Sumatra, Lampung, Kalimantan, West Java, Yogyakarta, and Nusa Tenggara [1,2]. In the South Sumatra region, the potential for iron sand is spread across several areas, such as Banyuasin, OKU, and Lahat, which have not been fully utilized optimally. Iron sand generally contains various iron oxide minerals such as magnetite (Fe_3O_4), hematite (Fe_2O_3), ilmenite ($FeTiO_3$), and quartz (SiO_2) [3,4]. The high content of Fe_3O_4 makes iron sand a potential raw material for the production of functional materials, including photocatalysts [1,5]. Several researchers have extracted Fe_3O_4 from Anoi Itam beach, Sabang [5], and Lampanah beach, Aceh [1]. However, studies focusing on the utilization of iron sand from South Sumatra, particularly from areas surrounding the Tekana River, remain limited. Therefore, exploring locally available iron sand as a precursor for Fe_3O_4-based photocatalysts is important to enhance resource utilization and support region-specific environmental applications.

Fe_3O_4 is a spinel-structured iron oxide with n-type semiconductor properties. The advantages of Fe_3O_4 as a photocatalyst are high saturation magnetization, chemical stability, low production costs, and low toxicity [6,7]. The low band gap energy value (<2.0 eV) can absorb the spectrum in both UV and visible light [6,8]. Extraction of Fe_3O_4 from iron sand can be done through coprecipitation, magnetic separation, and calcination methods. The method commonly used to synthesize Fe_3O_4 is coprecipitation, which is a precipitation reaction of iron salt solutions (Fe^{2+} and Fe^{3+}) in alkaline conditions [4,5]. The method is simple, does not require expensive equipment, and is able to produce Fe_3O_4 nanoparticles with small sizes and uniform distribution. The reaction can take place at low temperatures (usually <100 °C) and in a short time [9,10].

pH plays an important role in the success of Fe_3O_4 synthesis. The reaction pH can affect the size, morphology, and magnetization of Fe_3O_4. Increasing pH results in smaller particle sizes. At low pH, Fe_3O_4 nucleation growth is slow and produces particles that tend to be large. Conversely, at high pH, nucleation growth is fast, resulting in small particle sizes. However, if uncontrolled, further Fe^{2+} oxidation occurs. The synthesis of Fe_3O_4 carried out by Costa et at. a pH range (9.06, pH 12.75) produced various iron oxide phases such as magnetite, maghemite, and hematite [11]. It has been verified that with increasing pH value, the particle size decreases (from 53.53 nm to 9.49 nm). Likewise, research conducted by Rafie et al. showed that increasing pH resulted in smaller particle sizes, where in the photocatalytic application of Methylene blue dye, Fe_3O_4 synthesized at pH 11 had the greatest adsorption capacity compared to pH 10 and [12] .

This study aims to synthesize Fe_3O_4 from iron sand as a photocatalyst for Congo red dye (CRD). This dye has a molecular formula of $C_{32}H_{22}N_6Na_2O_6S_2$, belongs to the azo dye group (-N=N-), which has high chemical stability, so it is persistent in the environment and has the potential to cause toxic effects at various trophic levels [13,14]. In the CRD photodegradation process, Fe_3O_4 can absorb radiation energy and trigger the formation of highly reactive •OH and $•O_2^-$ radicals, thus capable of damaging the azo bonds and aromatic rings that make up the dye molecule [15,16]. Thus, research on the utilization of iron sand-based Fe_3O_4 for CRD photodegradation not only provides a more efficient and sustainable waste treatment solution but also supports the optimization of local mineral resources.

The photodegradation optimization process was conducted using the Response surface methodology (RSM) approach, which allows for simultaneous analysis of the influence and interaction of several variables with a more efficient number of experiments compared to conventional methods. The use of RSM also allows for more accurate prediction of optimum degradation conditions [17]. In addition, phytotoxicity testing was conducted to evaluate the safety level of the degradation solution, so that the effectiveness and environmental impact of the photocatalytic process can be comprehensively assessed.

MATERIALS AND METHODS

Materials

Iron sand was taken from the Tekana River, OKU, South Sumatra. Chemicals included HCl, NaOH, $NaNO_3$, NaOCl, and Congo red dye from Merck, Germany. *Vigna radiata* seeds were used for phytotoxicity testing. Distilled water were used as the reagents solvent.

Iron sand preparation

Iron sand was collected from the Tekana River, cleaned of impurities, and washed with distilled water until the water ran clear. It was then dried in the sun for one day. The iron sand was separated from the soil by attaching it to a magnet. The iron sand was then ground to a 100-mesh size [6,18].

Synthesis of Fe_3O_4

A total of 20 g of iron sand powder was mixed with 50 mL of HCl 1 N. The mixture was stirred with a magnetic stirrer at 800 rpm, and heated at 80 °C for 30 min. After the iron sand dissolved, the solution was filtered. The filtrate was added to a 2 M NaOH solution little by little with variations in the final pH (9, 10, and 11). The precipitate formed was washed several times with distilled water and ethanol until the pH was neutral. The precipitate was dried in an oven at 100 °C for 1 hour [6,18].

Characterization

The synthesized Fe_3O_4 was characterized using X-ray diffraction (XRD PANalytical) to determine the phase and crystal size at 2θ = 10-100°. Vibrating sample magnetometer (VSM OXFORD 1.2H) to determine the magnetic properties. Scanning electron microscopy with energy dispersive X-ray spectroscopy (SEM-EDX Tescan VEGA) to determine the morphology and elemental composition. Measurement of CRD concentration using a UV-Vis spectrophotometer (UH 5300, Hitachi)..

Determination of pHpzc

A total of 0.05 g of Fe_3O_4 was placed in an Erlenmeyer flask containing 25 mL of 0.1 M $NaNO_3$ solution. The pH was adjusted between 2 and 12 using 0.1 M NaOH and HCl solutions. The mixture was stirred at 200 rpm for 2 h and then allowed to stand for 24 h. The pHpzc was determined from the ΔpH (final pH-initial pH) versus initial pH graph [6].

Optimization photocatalytic degradation of CRD

Response surface methodology (RSM) was used to optimize photocatalytic degradation. Three independent variables were tested: pH (4-7), CRD concentration (10-40 mg/L), and irradiation time (30-90 min) using a Central composite design (CCD) and the Design Expert application. The mixture was stirred in the dark for 30 min before irradiation to reach equilibrium. Degradation was performed using visible light from a 150-watt (xenon lamp) at a distance of approximately 30 cm from the solution. The CRD volume used was 50 mL with a Fe_3O_4 mass of 0.1 g.

Phytotoxicity test

The phytotoxicity test was conducted using *Vigna radiata* seeds. A 15 mg/L CRD solution, a degraded CRD solution of the same concentration, and a control (distilled water), as well as 10 mL of the degraded solution, were added to germination trays containing cotton as a growth medium. *Vigna radiata* seeds were soaked in a 5% NaOCl solution for 10 min, then washed with distilled water to avoid microbial contamination. Thirty *Vigna radiata* seeds were placed in each tray. The trays were placed in a dark room at (±25 °C) for 48 h for initial germination. They were then grown outdoors for 5 days [19].

RESULTS AND DISCUSSION

Characterization of Fe_3O_4

In the process of extracting Fe_3O_4 from iron sand, HCl functions as a solvent that converts iron oxide compounds into chloride salts that are easily soluble in water. The mechanism involves a reaction between Fe_3O_4 and HCl, in which Fe^{2+} and Fe^{3+} ions are released into solution as $FeCl_2$ and $FeCl_3$. In general, the reaction occurs in two stages: first, H^+ ions from HCl attack and break the Fe–O bonds in the oxide structure, then Cl^- ions play a role in stabilizing the Fe ions in the form of chloride complexes. The reaction that occurs can be described as follows:

$$Fe_3O_4 + 8HCl \rightarrow FeCl_2 + 2FeCl_3 + 4H_2O \quad \ldots\ldots\ldots\ldots (1)$$

In the synthesis of Fe_3O_4, pH is an important parameter that determines the phase and size of the Fe_3O_4 crystals produced. The XRD spectra of Fe_3O_4 from iron sand synthesized at pH 9, 10, and 11 are presented in **Figure 1**. The three Fe_3O_4 spectra have the same pattern, according to ICDD No. 19-0529, namely at 2θ = 30, 35, 42, 53, 57, 62, and 74° corresponding to the crystal planes (220), (311), (400), (422), (511), (440), and (533). The main characteristic of the Fe_3O_4 XRD spectra is the highest peak at an angle of 2θ around 35°. It can be seen that increasing pH results in higher and sharper peak intensity.

Under strong base conditions, the precipitation of Fe^{2+} and Fe^{3+} ions occurs optimally so that a stable magnetite phase is formed, characterized by a sharp XRD pattern. At low pH, Fe^{2+} tends to oxidize to Fe^{3+} so that the formation of magnetite is imperfect and produces other phases such as α-Fe_2O_3, γ-Fe_2O_3, or FeOOH [20]. This can be seen from the XRD spectra in the form of weakened and widened peaks. pH also affects crystallite size, higher pH levels lead to improved crystal growth, resulting in narrower XRD peaks, whereas lower pH levels generally yield smaller and less uniform crystallites.

The findings are consistent with previous studies in which Fe_3O_4 was synthesized using $FeCl_3 \cdot 6H_2O$ and $FeCl_2 \cdot 4H_2O$ precursors at pH values of 10, 11, and 12. The results indicated that higher synthesis pH led to XRD patterns with increased intensity and sharper peaks, suggesting a reduction in crystallite size as the pH increased [18]. In the present study, the average crystallite sizes at pH 9, 10, and 11 were found to be 44.5, 35.6, and 28.4 nm, respectively. This trend confirms that alkaline conditions play a significant role in controlling crystal growth during the Fe_3O_4 synthesis.

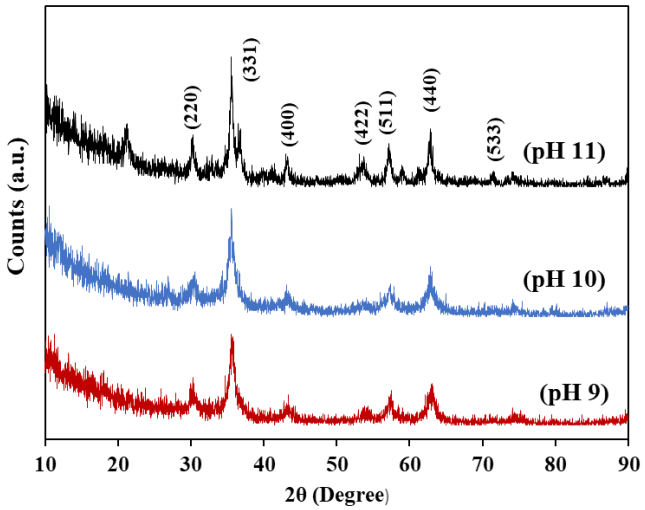

Figure 1. The XRD spectra of Fe_3O_4 synthesized at pH 9, 10, and 11

Magnetic properties provide advantages, especially the ease of separation of materials from solutions using magnets, and increased reuse efficiency. Fe_3O_4 exhibits superparamagnetic properties, which are easily magnetized when given a magnetic field but leave no residual magnetization after the field is removed. The specific saturation magnetization (Ms) value of Fe_3O_4 (bulk) is 92 emu/g [16]. In this study, Fe_3O_4 synthesized at pH 9, 10, and 11 had specific Ms of 58.97, 68.94, and 74.66 emu/g (**Figure 2**). The study conducted by Costa et al., the synthesis of Fe_3O_4 exhibited a similar trend whereas increasing the pH of hydrothermal synthesis of Fe_3O_4 increased the Ms value of Fe_3O_4, namely the lowest Ms value of 39.46 emu/g at pH 9.06 and the highest of 70.43 emu/g at pH 12.75 emu/g [20].

Based on the evaluation of the XRD spectra and saturation magnetization values, the Fe_3O_4 synthesized at pH 11 was selected for further morphological characterization using SEM-EDX, as shown in **Figure 3**. Fe_3O_4 particles appear close to each other and form large aggregates, which is a general characteristic of magnetic materials due to the attractive force between Fe_3O_4 particles. The Fe_3O_4 particles' shapes are a combination of square, oval, rod, and rectangular shapes [21]. This aggregate structure shows a fairly rough and inhomogeneous surface, which indicates the presence of nucleation and crystal growth processes that occur rapidly during synthesis. The results of EDX analysis show the content of Fe and O elements, which indicates the success of the synthesis, because there are no impurities. The composition of Fe and O is 71.54% and 28.46%, respectively.

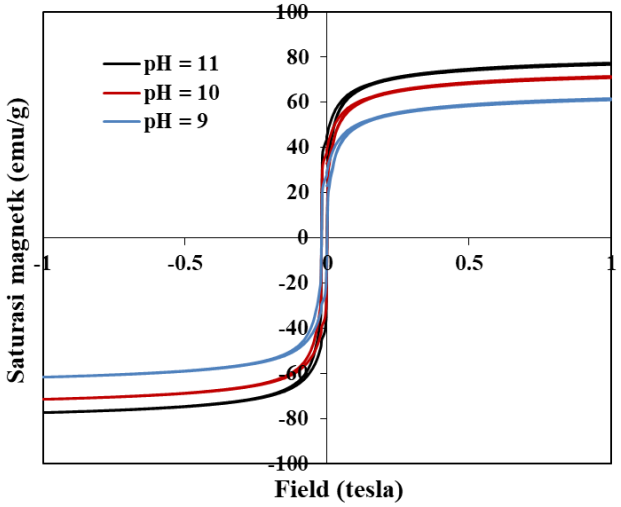

Figure 2. Saturation magnetization of Fe_3O_4 synthesized at pH 9, 10, and 11

Optimization of CRD degradation

Fe_3O_4 synthesized at pH 11 was used for the photocatalytic degradation of CRD. Optimization of photocatalytic degradation used RSM, an empirical modeling technique to investigate the relationship between experimental results and predictions [22]. **Table 1** shows the removal percentage for 3 variables, namely solution pH (A), CRD concentration (B), and irradiation time (C). The difference between the experimental and predicted degradation percentages ranged from 0.02 to 5.19. The small difference indicates that the model is able to predict the response well. **Figure 4** shows the relationship between actual and predicted for degradation efficiency. The points approaching the diagonal line indicate that the predicted value ≈ actual value. In addition, the alignment of the actual values along the straight line shows the agreement between the predicted and actual values, indicating that the model is accurate.

From the Analysis of variance (ANOVA) analysis results, the recommended model for statistical calculations is a quadratic polynomial model. The analysis results also showed that the obtained model

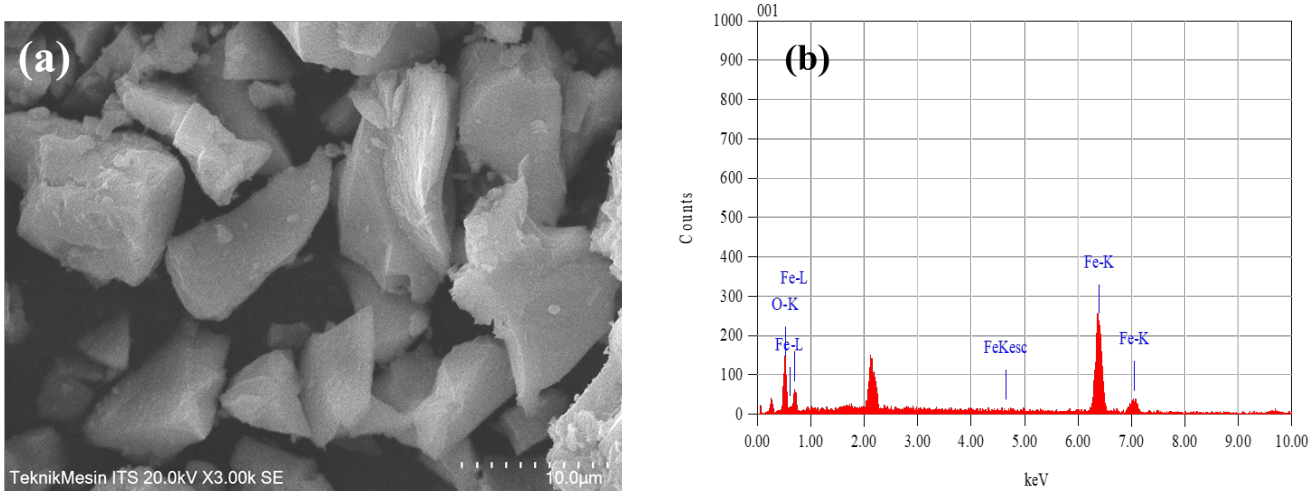

Figure 3. SEM image (a) and EDX spectra of Fe_3O_4 synthesized at pH 11 (b)

was statistically significant with an F-value of 50.66 and a p-value <0.0001. Models and variables with high F-values and low p-values (<0.05) are considered significant. This indicates that the developed model is able to explain the relationship between the independent variables and the response very well (**Table 2**). The main variables (A, B, and C) and interactions between variables have a significant effect because all have p-values <0.05. The lack of fit value is not significant (p = 0.0832 > 0.05), confirming that there is no systematic deviation between the model and the actual data. The residual value is relatively small (128.49) compared to the total variation (5986.30). This indicates that most of the data variation has been explained by the model. The quadratic model to describe the efficiency of CRD photocatalytic degradation by Fe_3O_4 is expressed in the following equation:

$$D(\%) = -51.56789 + 3.90678A + 4.98641B + 2.33072C - 0.139056AB + 0.080806AC - 0.016103BC - 0.474118A^2 - 0.047805B^2 - 0.021474C^2 \quad \text{.....(2)}$$

In the equation, positive (+) and negative (-) signs indicate the direction of the variable's influence on the response. A positive sign indicates a synergistic effect that supports increased CRD reduction, while a negative sign indicates the opposite effect.

Table 3 shows that the R^2 value = 0.9785 indicates that only about 2.15% is influenced by other factors (noise). The Adjusted R^2 value = 0.9592, not far from R^2, indicates that the model is not overfitting. The difference between the Predicted R^2 value = 0.8358 and Adjusted R^2 = 0.9592, of 0.1234 (<0.2), indicates that the model has good predictive ability. The C.V. value = 4.59%, which indicates that the experimental data have good reproducibility.

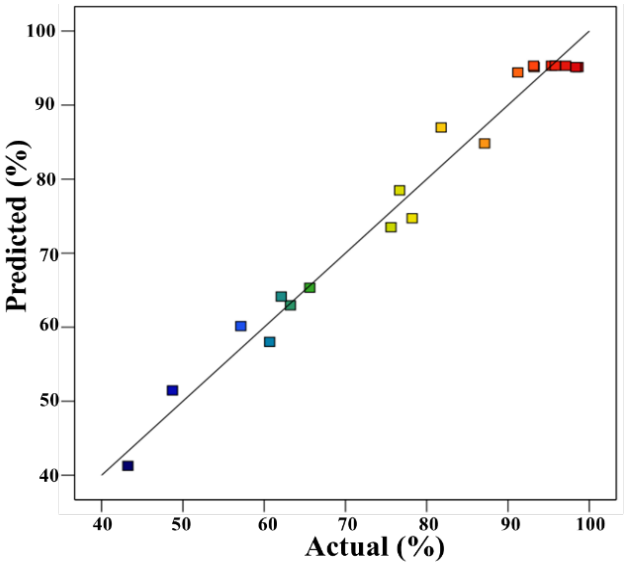

Figure 4. Plot of actual versus predicted CRD degradation efficiency

Table 3. Statistical adjustment for CRD removal

Parameters	Value
R^2	0.9785
Adjusted R^2	0.9592
Predicted R^2	0.8358
Adeq Precision	21.3226
Std. Dev	3.58
Mean	78.14
C.V. %	4.59

Degradation efficiency is influenced by the interaction between the dye and Fe_3O_4. The adsorption process is the initial step before degradation occurs.

Table 1. CCD design for 3 degradation variables

Run	pH	Concentration (mg/L)	Irradiation time (min)	Efficiency (%)		Residual
				Experiment	Predicted	
1	10	40	30	63.23	62.95	0.28
2	4	40	90	62.10	64.14	2.04
3	10	10	90	65.61	65.33	0.28
4	7	25	60	97.10	95.32	1.78
5	4	25	60	98.60	95.13	3.47
6	7	40	30	87.12	84.82	2.30
7	7	10	90	57.13	60.14	3.01
8	7	25	60	95.34	95.32	0.02
9	10	40	90	60.68	58.02	2.66
10	7	25	60	95.81	95.32	0.49
11	7	25	90	75.61	73.50	2.11
12	7	25	60	93.14	95.32	2.18
13	4	25	60	98.34	95.13	3.21
14	10	10	30	43.24	41.27	1.97
15	4	25	60	93.22	95.18	1.96
16	4	10	30	48.72	51.46	2.74
17	10	25	60	81.78	86.97	5.19
18	7	10	60	78.21	74.71	3.50
19	7	25	30	76.67	78.48	1.81
20	7	40	60	91.21	94.41	3.20

Table 2. ANOVA analysis for the quadratic model

Source	Sum of squares	Df	Mean square	F-Value	p-value	
Model	5857.81	9	650.87	50.66	< 0.0001	Significant
A. pH	727.52	1	141.27	10.99	0.0078	
B. Concentration	46.54	1	727.52	56.62	0.0462	
C. Irrad. time	46.54	1	46.54	3.62	0.0073	
AB	144.58	1	144.58	11.25	0.0030	
AC	195.28	1	195.28	15.20	0.0004	
BC	357.05	1	357.05	27.79	0.0340	
A^2	77.38	1	77.38	6.02	0.0004	
B^2	357.60	1	357.60	27.38	< 0.0001	
C^2	1154.46	1	1154.46	89.85		
Residual	128.49	10	12.85			
Lack of Fit	101.92	5	20.38	3.83	0.0832	Not significant
Pure error	26.57	5	5.31			
Cor Total	5986.30	19				

This interaction is influenced by the pH of the solution. pHpzc is the pH at which a material is neutrally charged. The pHpzc of Fe_3O_4 is 7.10 (**Figure 5**). Above pHpzc, the surface of materials will be negatively charged, while below pHpzc, the surface will be positively charged [23].

In this study, the optimum pH was obtained at pH < pHpzc. CRD is an anionic dye (negatively charged), while the Fe_3O_4 surface at pH < pHpzc is positively charged, resulting in more effective electrostatic interactions. Similar results were obtained for CRD degradation using ZnO NPS at pH 4.03 [24] and using In_2O_3 at pH 4 [14].

The 3D contour and surface graphs of CRD degradation are shown in **Figure 6**. The optimal condition is indicated by the light blue curved peak region. For example, an increase in concentration initially increases degradation efficiency. However, beyond a certain level, efficiency begins to decline, as reflected by the transition to darker blue areas. This phenomenon can be explained by the fact that at high CRD concentrations, the solution becomes more

concentrated, inhibiting light penetration, ultimately reducing degradation efficiency [25].

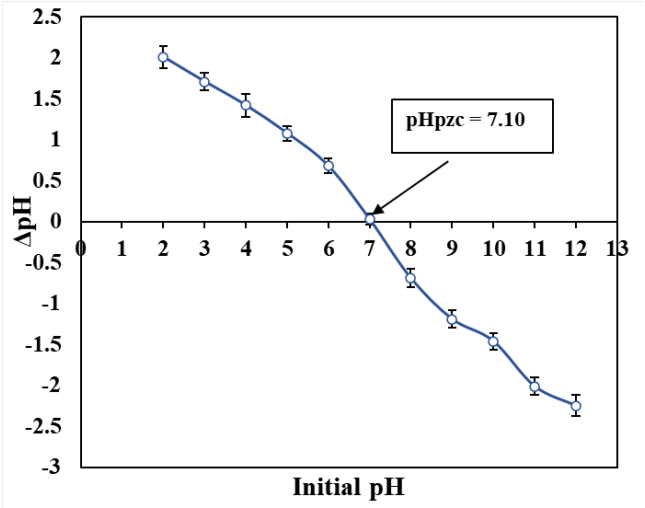

Figure 5. pHpzc of Fe_3O_4

Similarly, irradiation time influences degradation efficiency. In general, increasing irradiation duration increases degradation efficiency because more photons are absorbed by the catalyst to generate active radicals (such as •OH) [26]. However, after reaching the optimum time, increasing irradiation no longer provides significant improvements and may even lead to a decrease in efficiency due to electron-hole pair recombination or a reduction in the number of CRD molecules remaining to be degraded.

Table 4. Comparison between Experimental and Predicted Optimum Conditions

	Experimental	Predicted
A. pH	4.0	4.0
B. CRD (mg/L)	25	37.5
C. Irrad. time (min)	60	62
Degradation (%)	98.60	98.93

The optimal conditions for the photocatalytic degradation of CRD using Fe_3O_4, as determined by RSM, along with the experimental results, are presented in **Table 4**. Notable differences were observed under nearly identical irradiation times of approximately 60 min. The predicted model indicated the capability to degrade a higher CRD concentration of 37.5 mg/L, whereas the experimental result achieved degradation at 25 mg/L, albeit with greater degradation efficiency. This discrepancy suggests that while the RSM model effectively predicts experimental conditions, it may provide better degradation performance.

The desirability value (d) indicates the level of desirability of a response, where d = 0 means undesirable and d = 1 indicates the most optimal condition. Desirability value of 1 indicates that the optimization process has successfully identified conditions that fully satisfy all the set criteria and objectives within the RSM model [22]. This means that the selected combination of variables, including pH, CRD concentration, and irradiation time, represents the most optimal condition for achieving maximum degradation efficiency (**Figure 7**). There is no compromise between the response variables, and the system operates at its highest predicted performance.

Reusability study

The durability and reusability of photocatalysts play a crucial role in determining their suitability for environmental remediation in industry [25]. Fe_3O_4 was separated from the solution by centrifugation, then washed with distilled water and methanol, dried, and reused for photodegradation [26]. **Figure 8** shows the reusability of the catalyst during five cycles conducted under optimum conditions: pH = 4.0, CRD concentration of 37.5 mg/L, and irradiation time of 62 min. During the five cycles, degradation efficiency decreased by 6.91%, although the catalyst maintained high photocatalytic activity (> 90% degradation efficiency). This decrease could be due to structural changes or the adsorption of degradation byproducts [27]. This indicates good stability and reusability. Another study, on the degradation of CRD using a 3 wt% rGO/LDH nanocomposite, found a 13% reduction in degradation efficiency during five reusability cycles [25].

The mechanism of photocatalytic degradation of CRD by Fe_3O_4 is explained as follows: when Fe_3O_4 is exposed to visible light, electron-hole pairs are formed due to the excitation of electrons (e^-) from the valence band to the conduction band. The resulting electrons then react with dissolved oxygen to form superoxide radicals ($•O_2^-$), while holes (h^+) interact with water molecules to produce hydroxyl radicals (•OH). The species ($•O_2^-$) and (•OH) are the main reactive species that convert organic contaminants into less hazardous substances such as CO_2 and H_2O, as well as other mineralization products. The degradation mechanism of CRD as follow: [21,28]

$Fe_3O_4 + h\nu \rightarrow eCB^- + hVB^+$ .....(3)
$eCB^- + O_2 \rightarrow •O_2^-$ .....(4)
$hVB^+ + OH^- \rightarrow •OH$ .....(5)
$hVB^+ + H_2O \rightarrow H^+ + •OH$ .....(6)
$•OH + •O_2^- + CRD \rightarrow H_2O + CO_2 +$ other product ..(7)

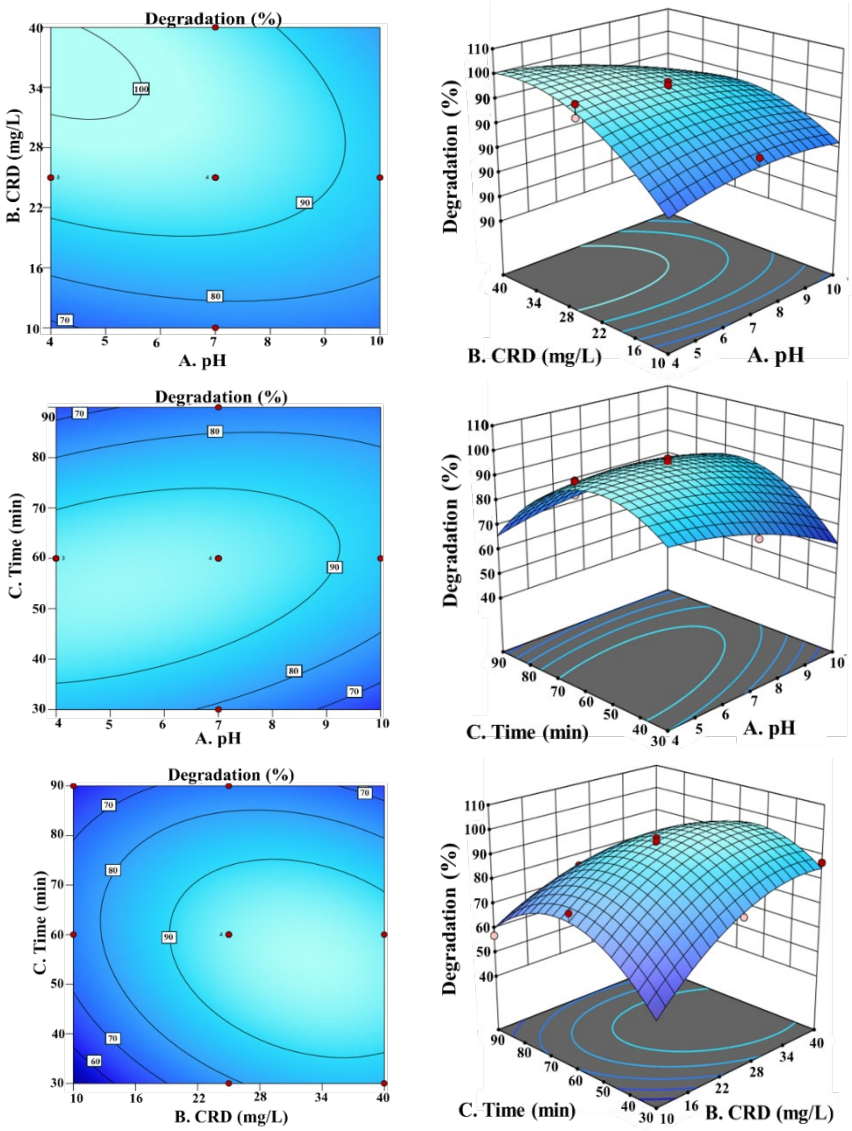

Figure 6. 3D surface visualizations and contour depicting CRD photodegradation by Fe_3O_4

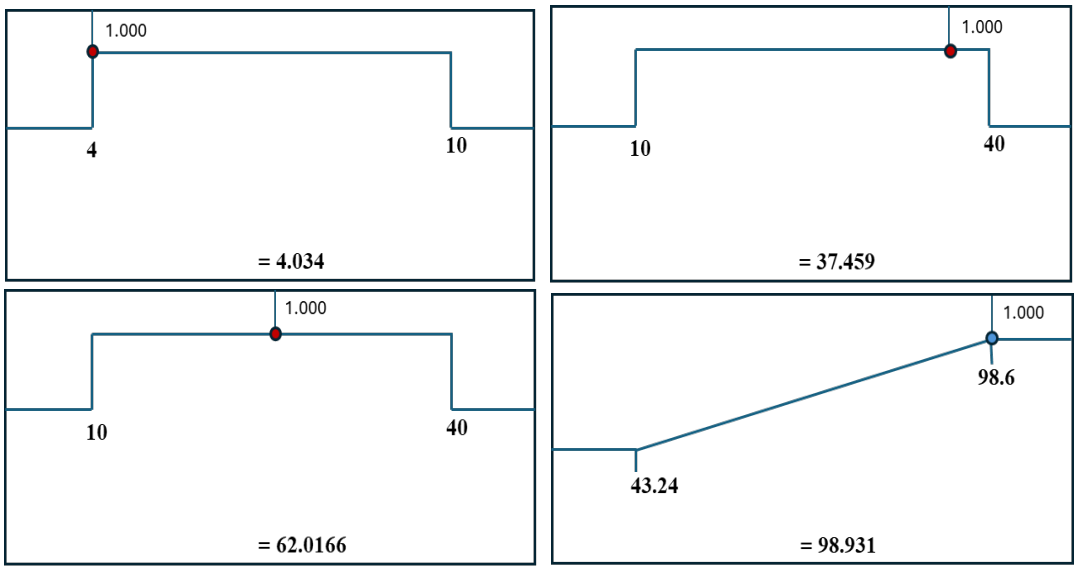

Figure 7. Desirability value at optimum conditions

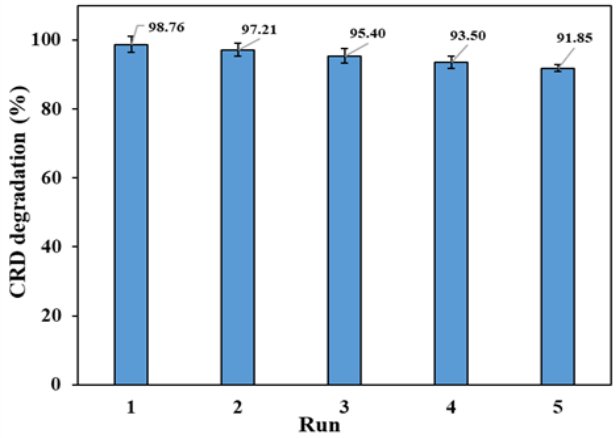

Figure 8. Recycling performance of Fe_3O_4 for CRD

Phytotoxicity study

Plants can be used as effective indicators to detect mutations caused by exposure to toxic substances in polluted environments and are therefore often used in hazard assessments [29]. Scientifically, roots serve as the primary indicator because they are the first part to come into direct contact with toxic substances and are highly sensitive to environmental changes [19]. Phytotoxicity testing in this study was conducted using *Vigna radiata* with three treatments: (i) dye non-treatment, (ii) degraded dye, and (iii) control. Germination rates were evaluated for five days, with stem length as the observation parameter. The results shown in **Figure 9** indicate that the degradation process effectively reduced dye toxicity, making it safer for plant growth. This is demonstrated by the lack of significant differences in mung bean growth between the degraded dye treatment and the control. Conversely, treatment with undegraded dye resulted in reduced germination and inhibited root and stem growth. Hamad et al. reported a comparable phenomenon, in which the germination rate of lentil plants exposed to CRD was lower than that observed in both the degradation products and the control treatment [30].

Figure 9. Phytotoxicity study of CRD on *Vigna radiata:* (i) CRD non-treatment (ii) CRD degraded, and (iii) control

CONCLUSION

The synthesis of Fe_3O_4 from iron sand of the Tekana River, OKU, South Sumatra, Indonesia, has been successful. The synthesis was carried out with variations in pH (9, 10, and 11) using the coprecipitation method. The results showed that increasing the synthesis pH was able to increase the magnetic properties and reduce the crystal size. The application of Fe_3O_4 synthesized at pH 11 as a catalyst in the degradation of Congo red dye (CRD), which was optimized using the Response surface methodology (RSM) method, resulted in a degradation efficiency of 98.93% (pH = 4.0; CRD concentration = 37.5 mg/L; and irradiation time = 62 min). In addition to high degradation efficiency, the performance of Fe_3O_4 as a good catalyst was demonstrated through reusability tests, where up to five degradation cycles resulted in a degradation efficiency above 90%, which decreased from 98.76% to 91.85%. In addition, the phytotoxicity test results showed that Fe_3O_4 is safe to use, indicated by the absence of significant differences in the growth of mung bean seeds using degraded CRD solution media and the control. Thus, Fe_3O_4 synthesized from iron sand has the potential as an economical, effective, and environmentally friendly catalyst.

REFERENCES

[1] B. Satria, Z. Masrurah, and S. J. Fajar, "Magnetic susceptibility and grain size distribution as prospective tools for selective exploration and provenance study of iron sand deposits: A case study from Aceh, Indonesia," *Heliyon*, vol. 7, no. 12, pp. 1-8, 2021.

[2] R. Prasetyowati, E. F. M. Harahap, R. I. Saputri, P. E. Swastika, F. F. Fauzi, Supardi, Warsono, Ariswan, and W. S. B. Swandaru, "Degradation of methyl orange dye using Fe_3O_4/GO photocatalyst with iron derived from coastal Glagah Kulon Progo ore," *Nano-Structures and Nano-Objects*, vol. 38, pp. 1-12, 2024.

[3] H. Heryanto and D. Tahir, "The correlations between structural and optical properties of magnetite nanoparticles synthesized from natural iron sand," *Ceramics International*, vol. 47, no. 12, pp. 16820–16827, 2021.

[4] G. H. Tamuntuan, A. Ardiansyah, A. D. Wuntu, G. Pasau, D. Darwis, D. Pandara, and D. Tahir, "Iron sand–derived materials: A review on synthesis routes, magnetic properties, and multifunctional applications," *Minerals Engineering*, vol. 240, pp. 1-18, 2026.

[5] S. Nengsih, S. Nur Abdulmadjid, M. Mursal, and Z. Jalil, "Photocatalytic performance of

Fe_3O_4-TiO_2 in the degradation of methylene blue dye: optimizing the usability of natural iron sand," *Materials Science for Energy Technologies*, vol. 7, pp. 374-380, 2024.

[6] P. L. Hariani, S. Salni, M. Said, and R. Farahdiba, "Core-shell $Fe_3O_4/SiO_2/TiO_2$ magnetic modified Ag for the photocatalytic degradation of Congo red dye and antibacterial activity," *Bulletin of Chemical Reaction Engineering and Catalysis*, vol. 18, no. 2, pp. 315–330, 2023.

[7] M. M. Ba-Abbad, A. Benamour, D. Ewis, A. W. Mohammad, and E. Mahmoudi, "Synthesis of Fe_3O_4 nanoparticles with different shapes through a co-precipitation method and their application," *Journal of The Minerals, Metals & Materials Society*, vol. 74, no. 9, pp. 3531–3539, 2022.

[8] N. Madima, K. K. Kefeni, S. B. Mishra, A. K. Mishra, and A. T. Kuvarega, "Fabrication of magnetic recoverable Fe_3O_4/TiO_2 heterostructure for photocatalytic degradation of Rhodamine B dye," *Inorganic Chemistry Communications*, vol. 145, pp. 1-13, 2022.

[9] S. Liu, B. Yu, S. Wang, Y. Shen, and H. Cong, "Preparation, surface functionalization and application of Fe_3O_4 magnetic nanoparticles," *Advances in Colloid and Interface Science*, vol. 281, pp. 1-30, 2020.

[10] S. Katiyar and R. Katiyar, "Eco-friendly Fe_3O_4-biochar nanocomposite from sawdust for efficient chromium removal: A study on adsorption of Cr(VI)," *Journal of the Indian Chemical Society*, vol. 102, no. 12, pp. 1-17, 2025.

[11] B. Costa, E. Pereira, V. C. Ferreira-Filho, A. S. Pires, L. C. J. Pereira, P. I. P. Soares, M. F. Botelho, F. Mendes, M. P. F. Graca, and S. S. Teixeira, "Influence of the pH synthesis of Fe_3O_4 magnetic nanoparticles on their applicability for magnetic hyperthermia: an in vitro analysis," *Pharmaceutics*, vol. 17, no. 7, pp. 1-18, 2025.

[12] S. F. Rafie, H. Sayahi, H. Abdollahi, and N. Abu-Zahra, "Hydrothermal synthesis of Fe_3O_4 nanoparticles at different pHs and its effect on discoloration of methylene blue: Evaluation of alternatives by TOPSIS method," *Materials Today Communications*, vol. 37, pp. 1-17, 2023.

[13] A. Herawati, R. M. Aryani, G. Antarnusa, Khoiriah, and A. Nene, "Fe_3O_4/chitosan nanocomposites for Congo red removal: Adsorption surpasses photodegradation," *Materials Chemistry and Physics*, vol. 347, pp. 1-17, 2026.

[14] S. I. Siddiqui, E. S. Allehyani, A. A. Al-Harbi, Z. Hasan, M. A. Abomuti, H. K. Rajor, and S. Oh, "Investigation of Congo red toxicity towards different living organisms: A Review," *Processes*, vol. 11, pp. 1-12, 2023.

[15] D. Arockia Jency, K. Sathyavathi, M. Umadevi, and R. Parimaladevi, "Enhanced bioactivity of Fe_3O_4-Au nanocomposites – A comparative antibacterial study," *Materials Letters*, vol. 258, pp. 1-4, 2020.

[16] M. Kohale, H. Inamdar, K. Kokate, R. Ingale, J. Joshi, D. Singh, A. Katti, S. Polshettiwar, R. Aher, and S. Kulkarni, "Engineering magnetite (Fe_3O_4) nanoparticles: controlled synthesis, surface functionalization, and multidisciplinary technological applications: A Review," *Progress in Crystal Growth and Characterization Materials*, vol. 15, pp. 1-39, 2026.

[17] M. Afaq, A. Sajid, Q. Manzoor, F. Imtiaz, A. Sajid, R. Javed, A. Ahmad, N. Alwadai, W. Mnif, and M. Igbal, "Sonochemical synthesis of CoO-ZnO nanocomposite and optimizing the degradation of toxic anionic dye using RSM-BBD," *Materials Science and Engineering: B*, vol. 312, pp. 1-10, 2025.

[18] S. S. N. Nengsih, M. Abdulmadjid, R. Mursal, Idroes, and Z. Jalil, "Magnetization study iron sand from Sabang, Indonesia: the potential of magnetic materials in the photocatalytic field," *Bulletin of Chemical Reaction Engineering & Catalysis*, vol. 18, no. 2, pp. 344-35, 2023.

[19] S. Abhirami, G. Thiruppathi, M. S. Ola, M. Arunkumar, P. Sundararaj, and P. V. Joseph, "Eco-conscious synthesis of chitosan-reduced magnetic Iron oxide nanocomposite from crab Shell waste for photocatalytic degradation of textile dyes: Ecotoxicity insights," *Journal of Water Process Engineering*, vol. 78, pp. 1-13, 2025.

[20] Z. S. Gano, E. A. Audu, A. A. Osigbesan, A. F. Ade-Ajayi, and J. T. Barminas, "Novel mesoporous iron oxide synthesized from naturally occurring magnetic sand: a potential and promising catalyst for chemical processes," *Inorganic Chemistry Communications*, vol. 159, pp. 1-8, 2024.

[21] T. B. Mbuyazi and P. A. Ajibade, "Photocatalytic degradation of organic dyes by magnetite nanoparticles prepared by Co-precipitation," *International Journal of*

Molecular Sciences, vol. 25, no. 14, pp. 1-18, 2024.

[22] H. Gomaa, Y. Zhai, T. Wang, C. An, A. Lee, Q. Deng, and N. Hu, "Morphology-performance relationship in hollow-sphere cobalt sulfide photocatalysts for solar-light-driven dye degradation: integration of RSM, DFT, and machine learning," *Journal of Environmental Chemical Engineering*, vol. 13, no. 6, pp. 1-19, 2025.

[23] K. Subramani, J. K. S. Ganeshan, S. Srinivasan, N. V. T. Mohanasundaram, and A. Incharoensakdi, "Hydrothermally and green synthesized TiO_2 nanoparticles with high photocatalytic textile industry dye degradation, antibacterial and antioxidant activities," *Journal of Alloys and Compounds*, vol. 1017, pp. 1-16, 2025.

[24] R. Moeinzadeh, N. Azizi, M. Hekmati, M. Qomi, and D. Esmaeili, "ZnONPs/covalent triazine frameworks nanocomposite as high-performance photocatalysts for degradation of Congo red under visible light," *Materials Chemistry and Physics*, vol. 307, pp. 1-12, 2023.

[25] D. Mahar, N. Semwal, T. Arya, and M. C. Arya, "Facile hydrothermal fabrication and performance tuning of rGO/LDH nanocomposites for efficient photocatalytic degradation of Congo red," *Journal of Hazardous Materials Advances*, vol. 21, pp. 1-19, 2026.

[26] N. Khera and P. Jeevanandam, "Core-shell composite nanoarchitectonics of TiO_2@$NiCo_2S_4$ via thermal decomposition approach for photodegradation of Congo red," *Environmental Research*, vol. 274, pp. 1-7, 2025.

[27] L. R. Buddiga, G. R. Gajula, and G. Jaishree, "Methyl orange dye degradation of dual doped TiO_2 nanoparticles under visible light Irradiation," *Journal of the Indian Chemical Society*, vol. 102, no. 9, pp. 1-14, 2025.

[28] H. Madhu and S. R. Prasad, "Synthesis and characterization of $MnFe_2O_4$ and Clay/$MnFe_2O_4$ using neem leaves for photodegradation and radical scavenging studies," *Sustainable Chemistry One World*, vol. 7, pp. 1-12, 2025.

[29] G. Sofia, C. Koventhan, S. Kanmani, and A. Y. Lo, "Green synthesized rGO/TiO_2/g-C_3N_4 nanocomposites via *Plectranthus amboinicus* extract for efficient photocatalytic degradation of methylene blue: RSM optimization, antimicrobial and phytotoxicity assessment," *Journal Environmental Chemical Engineering*, vol. 13, no. 1, pp. 1-16, 2025.

[30] M. T. M. H. Hamad and M. S. S. Saied, "Kinetic studies of Congo red dye adsorption by immobilized Aspergillus niger on alginate," *Applied Water Science*, vol. 11, no. 35, pp. 1-12, 2021.